JOURNAL OF THE AMERICAN WATER RESOURCES ASSOCIATION
Vol. 52, No. 5 AMERICAN WATER RESOURCES ASSOCIATION October 2016

THE INFLUENCE OF THE PACIFIC DECADAL OSCILLATION ON ANNUAL FLOODS IN THE RIVERS OF WESTERN CANADA[1]

Sunil Gurrapu, Jeannine-Marie St-Jacques, David J. Sauchyn, and Kyle R. Hodder[2]

ABSTRACT: We analyzed annual peak flow series from 127 naturally flowing or naturalized streamflow gauges across western Canada to examine the impact of the Pacific Decadal Oscillation (PDO) on annual flood risk, which has been previously unexamined in detail. Using Spearman's rank correlation ρ and permutation tests on quantile-quantile plots, we show that higher magnitude floods are more likely during the negative phase of the PDO than during the positive phase (shown at 38% of the stations by Spearman's rank correlations and at 51% of the stations according to the permutation tests). Flood frequency analysis (FFA) stratified according to PDO phase suggests that higher magnitude floods may also occur more frequently during the negative PDO phase than during the positive phase. Our results hold throughout much of this region, with the upper Fraser River Basin, the Columbia River Basin, and the North Saskatchewan River Basin particularly subject to this effect. Our results add to other researchers' work questioning the wholesale validity of the key assumption in FFA that the annual peak flow series at a site is independently and identically distributed. Hence, knowledge of large-scale climate state should be considered prior to the design and construction of infrastructure.

(KEY TERMS: Western Canada; floods; independently and identically distributed assumption (*i.i.d.*) of flood frequency analysis; multi-decadal variability; Pacific Decadal Oscillation; Fraser River Basin; Columbia River Basin; North Saskatchewan River Basin; permutation test for quantile-quantile plots.)

Gurrapu, Sunil, Jeannine-Marie St-Jacques, David J. Sauchyn, and Kyle R. Hodder, 2016. The Influence of the Pacific Decadal Oscillation on Annual Floods in the Rivers of Western Canada. *Journal of the American Water Resources Association* (JAWRA) 52(5):1031-1045. DOI: 10.1111/1752-1688.12433.

INTRODUCTION

Numerous studies have identified teleconnections between western Canadian hydroclimate and ocean-atmosphere oscillations such as the Pacific Decadal Oscillation (PDO) and the El Niño-Southern Oscillation (ENSO) (e.g., Shabbar and Khandekar, 1996; Shabbar *et al.*, 1997; Bonsal and Lawford, 1999; Rood *et al.*, 2005; Gobena and Gan, 2006; Bonsal and Shabbar, 2008; St. Jacques *et al.*, 2010, 2014; Whitfield *et al.*, 2010; Lapp *et al.*, 2013). Winters are typically cooler and wetter, with deeper snowpack, and annual discharge greater during the negative (cold) PDO phase and La Niña, whereas the positive (warm) PDO phase and El Niño produce generally warmer and drier winter months with less snowpack, and less annual discharge. However, despite these many studies of teleconnections and total annual discharge, there has not been as much work related to the magnitude and frequency of annual peak flows in the rivers of western Canada. Seminal work of Woo

[1]Paper No. JAWRA-15-0013-P of the *Journal of the American Water Resources Association* (JAWRA). Received January 29, 2015; accepted April 11, 2016. **Discussions are open until six months from issue publication.**

[2]PhD Candidate (Gurrapu), Adjunct Professor (St-Jacques), and Department Head and Associate Professor (Hodder), Department of Geography and Environmental Studies; Research Associate (St-Jacques) and Research Professor (Sauchyn), Prairie Adaptation Research Collaborative, University of Regina, 3737 Wascana Parkway, Regina, Saskatchewan S4S 0A2, Canada (E-Mail/ St-Jacques: jmcheval@sympatico.ca).

and Thorne (2003) showed that the high-frequency ENSO and the Pacific North American mode (PNA) have a significant influence on peak streamflows in western Canada, with peak flows being higher during La Niña events and when the PNA is in a negative state, and with peak flows being lower during El Niño events and when the PNA is in a positive state. However, no researchers have examined the effect of the low-frequency PDO on annual peak flows in western Canada.

In western Canada, the Fraser, Columbia, North Saskatchewan, South Saskatchewan, Peace, and Athabasca Rivers arise in the mountains from snowpack and flow through the provinces of British Columbia, Alberta, and Saskatchewan. The region has experienced devastating floods, causing much economic damage and creating a demand for the construction of flood-resistant infrastructure that is also respectful of the natural environment. For example, the May 1948 Vanport flood on the Fraser and Columbia Rivers extended throughout southern British Columbia (including Vancouver), Washington, and Oregon and caused over $100 million in infrastructure and property damage and killed 51 people. Presently in western Canada, there is a debate over whether the proposed Northern Gateway Pipeline (from near Edmonton, Alberta, through the upper Fraser River Valley, to a new marine terminal in Kitimat, British Columbia, for the exportation of petroleum) can be safely constructed through a pristine natural environment and First Nations territories (http://gateway-panel.review-examen.gc.ca/clf-nsi/dcmnt/rcmndtnsrprt/rcmndtnsrprtvlm2ppndx-eng.html). Regionally, there is a vast amount of infrastructure, including pipelines, already in place, possibly constructed according to unrealistic flood frequency scenarios.

Information concerning flood magnitude and frequency is vital in the optimal planning and design of reliable infrastructure. Flood frequency analysis (FFA) is widely used for effective planning and design of water resource and transportation infrastructure. A primary assumption in FFA is that the annual peak flow series at a site is independently and identically distributed (*i.i.d.*). This implies that the state of the relevant climate oscillations that are known to affect the regional hydroclimate can be ignored. However, research is questioning the validity of the *i.i.d.* assumption (e.g., Kwon *et al.*, 2008; Stedinger and Griffis, 2008, 2011; López and Francès, 2013; Barros *et al.*, 2014; Tan and Gan, 2015) and suggests that consequently, knowledge of large-scale climate state patterns should be considered when performing FFA.

In this study, we analyzed the annual peak flows of the rivers of western Canada with the hypothesis that they are influenced by the PDO. Our study was motivated by the observation that the influence of low-frequency climate oscillations such as the PDO upon annual flood risk across the region is not yet a key ingredient in the planning and design of regional infrastructure. It is the first to examine the impact of the PDO, which is known to be a major influence on annual mean streamflow (e.g., Mantua *et al.*, 1997; Rood *et al.*, 2005; Gobena and Gan, 2006; Wang *et al.*, 2006; Fleming *et al.*, 2007; Fleming and Whitfield, 2010; St. Jacques *et al.*, 2010, 2014; Whitfield *et al.*, 2010), on peak flow in the region. The necessity of such a study is illustrated by annual hydrographs of regional rivers which show higher peak flow during the negative PDO phase and lower peak flow during the positive PDO phase. For example, the annual discharge and the annual peak flow in Crowsnest River at Frank (WSC 05AA008) in 1956, the year with the lowest negative PDO index over 1901-2013, were substantially higher than those in 1987, the year with the highest positive PDO index (Figure 1).

STUDY AREA AND DATA

To evaluate the influence of the PDO on annual peak streamflow in the rivers of western Canada, we chose daily peak flow records from 119 naturally

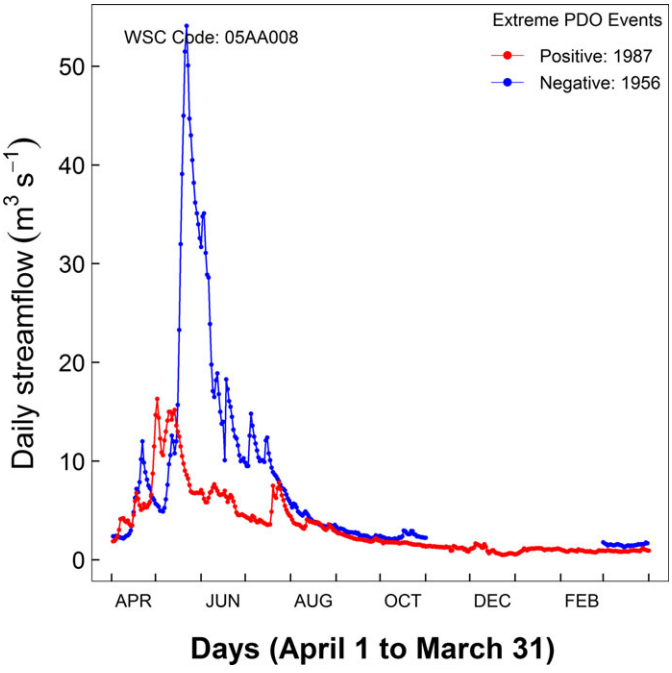

FIGURE 1. Response Hydrographs of the Crowsnest River at Frank (WSC 05AA008) for 1956, the Year with the Most Negative Pacific Decadal Oscillation (PDO) Index (−2.72; blue line), and for 1987, the Year with the Most Positive PDO Index (1.85; red line). The PDO index is averaged for November to March.

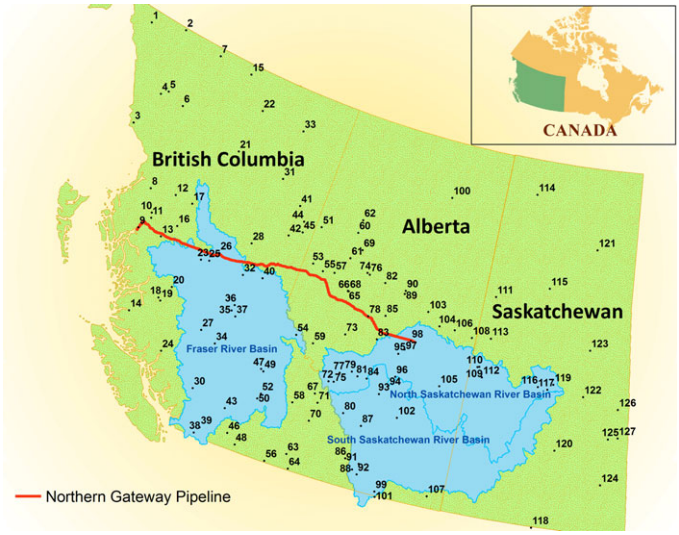

FIGURE 2. Locations of the Selected Streamflow Gauges on the Rivers of Western Canada from the Canadian Hydrometric Database (Water Survey of Canada; WSC). The gauges are numbered from west to east based on their longitude. Details of each station are listed in Table 1 and Table S1.

flowing streamflow gauges (Figure 2, Figure S1, Table 1, and Table S1) across British Columbia, Alberta, and Saskatchewan. The datasets were obtained from the Water Survey of Canada (WSC) database (Environment Canada, HYDAT Database, http://www.ec.gc.ca/rhc-wsc/default.asp?lang=En&n=9018B5EC-1). These stations were chosen based on the availability of long-term daily streamflow records. All the stations have at least 30 years of data, whether continuous or discontinuous. One hundred and ten of these stations were analyzed earlier by Woo and Thorne (2003) for the influence of ENSO and the PNA on the peak flows. In addition, eight naturalized records (two naturally flowing and six regulated) from the North Saskatchewan River Basin (NSRB), with weekly peak flows from Alberta Environment, were included in the analysis (http://esrd.alberta.ca/) (Figure 2, Figure S1, Table 1, and Table S1). These eight stations were included for additional spatial coverage and to examine continuous long-term data from this economically important watershed. The earliest of the 127 records begins in 1905 and the majority end in 2013. The 127 records have an average length of 52 years. The gross drainage area of the selected river basins ranges from 155 to 60,000 km^2. The majority of these rivers originate from snowmelt in the western Cordillera (Figure S1). Annual peak flow in these rivers typically occurs during the spring or early summer months from rapid snowmelt and precipitation as rain. The time series of annual peak flows at each station were extracted from the daily (weekly for the eight NSRB records) averaged streamflow records for the water year starting October 1st and ending on September 30th of the following year. For each gauge, peak flow data for any given year was included only if there were at most 10 missing days throughout spring (March-June).

To analyze the influence of the PDO on annual peak streamflow, we used the November to March monthly averaged PDO (Figure 3) index from the Joint Institute for the Study of Atmosphere and Ocean (JISAO), University of Washington (http://jisao.washington.edu/pdo/) (Mantua *et al.*, 1997). The annual peak flow series at each station was stratified based on the negative (cold: 1890-1924, 1947-1976, 2009-2013) and positive (warm: 1925-1946, 1977-2008) phases of the PDO (Mantua *et al.*, 1997; Minobe, 1997).

To directly compare the results from the low-frequency PDO to those from the higher frequency ENSO, we also analyzed the influence of ENSO on peak streamflow. The Southern Oscillation Index (SOI) was used to categorize ENSO events (Climate Research Unit, University of East Anglia, http://www.cru.uea.ac.uk/cru/data/soi/). We used the June to November averaged SOI, with the annual peak flows at the gauges stratified into El Niño (SOI ≤ -0.5), La Niña (SOI ≥ 0.5), or neutral-year ($-0.5 <$ SOI < 0.5) flows based on the previous year's SOI (Table 2 and Figure S2), because ENSO's impact on the Pacific Northwest is lagged by a year (Redmond and Koch, 1991).

METHODS

First, to explore whether the magnitude of annual peak flows are related to the large-scale climate oscillations, we computed the nonparametric Spearman's rank correlation coefficient (ρ) to measure the strength of the correlation between the annual peak flows and the PDO index or SOI at each of the 127 gauges. Spearman's coefficient was used because it is robust and is not affected by the distribution of the climate and hydrologic data (Woo and Thorne, 2003; Wilks, 2006). In this analysis, any rank correlation ρ with p-value ≤ 0.1 is considered significant. We used the full period of record throughout this study because it is the longest record lengths that enable detection of the impact of the low-frequency PDO.

To further explore if the peak flows stratified according to PDO phase came from the same population, we ranked the peak flow series of each phase of the PDO and created quantile-quantile (Q-Q) plots

TABLE 1. List of the 127 Selected Streamflow Gauges from the Canadian Hydrometric Database (Water Survey of Canada-WSC), with Their WSC Code, Drainage Area (km^2), and Location. Full details of these gauge records are in Table S1.

ID	WSC Code	Gauge Name	Province	Drainage Area	Latitude	Longitude
1	09AA006	Atlin River near Atlin	BC	6,860	59.595	−133.814
2	09AE003	Swift River near Swift River	BC	3,390	59.931	−131.768
3	08CG001	Iskut River below Johnson River	BC	9,500	56.739	−131.674
4	08CE001	Stikine River at Telegraph Creek	BC	29,000	57.901	−131.154
5	08CD001	Tuya River near Telegraph Creek	BC	3,550	58.072	−130.824
6	08CC001	Klappan River near Telegraph Creek	BC	3,550	57.900	−129.704
7	10AC004	Blue River near the mouth	BC	1,700	59.758	−129.128
8	08DB001	Nass River above Shumal Creek	BC	18,400	55.264	−129.086
9	08FF001	Kitimat River below Hirsch Creek	BC	1,990	54.049	−128.690
10	08EF001	Skeena River at Usk	BC	42,300	54.631	−128.432
11	08EF005	Zymoetz River above O.K. Creek	BC	2,850	54.483	−128.331
12	08EB004	Kispiox River near Hazelton	BC	1,880	55.434	−127.714
13	08ED002	Morice River near Houston	BC	1,900	54.118	−127.424
14	08FA002	Wannock River at outlet of Owikeno Lake	BC	3,900	51.679	−127.179
15	10BC001	Coal River at the mouth	BC	9,190	59.691	−126.951
16	08EE004	Bulkley River at Quick	BC	7,340	54.618	−126.899
17	08EC013	Babine River at outlet of Nolkitkwa Lake	BC	6,760	55.425	−126.703
18	08FB007	Bella Coola River above Burnt Bridge Creek	BC	3,720	52.422	−126.158
19	08FB006	Atnarko River near the mouth	BC	2,550	52.361	−126.006
20	08FC003	Dean River below Tanswanket Creek	BC	3,720	52.890	−125.771
21	07EA002	Kwadacha River near Ware	BC	2,410	57.450	−125.638
22	10BE004	Toad River above Nonda Creek	BC	2,540	58.855	−125.383
23	08JB002	Stellako River at Glenannan	BC	3,600	54.008	−125.009
24	08GD004	Homathko River near Fort Fraser	BC	5,680	50.990	−124.918
25	08JB003	Nautley River near Fort Fraser	BC	6,030	54.085	−124.599
26	08JE001	Stuart River near Fort St. James	BC	14,200	54.418	−124.275
27	08MA001	Chilko River near Redstone	BC	6,880	52.070	−123.537
28	07EE007	Parnsip River above Misinchinka River	BC	4,930	55.078	−122.905
29	08KG001	West Road River near Cinema	BC	12,400	53.311	−122.888
30	08MG005	Lillooet River near Pemberton	BC	2,100	50.336	−122.799
31	10CB001	Sikanni Chief River near Fort Nelson	BC	2,180	57.234	−122.694
32	08KC001	Salmon River near Prince George	BC	4,230	54.096	−122.678
33	10CD001	Muskwa River near Fort Nelson	BC	20,300	58.788	−122.659
34	08MB005	Chilcotin River below Big Creek	BC	19,200	51.849	−122.653
35	08KE016	Baker Creek at Quesnel	BC	1,550	52.973	−122.520
36	08KE009	Cottonwood River near Cinema	BC	1,910	53.155	−122.476
37	08KH006	Quesnel River near Quesnel	BC	11,500	52.844	−122.224
38	08MH001	Chilliwack River at Vedder Crossing	BC	1,230	49.097	−121.963
39	08MG013	Harrison River near Harrison Hot Springs	BC	7,890	49.311	−121.802
40	08KB003	McGregor River at Lower Canyon	BC	4,780	54.231	−121.669
41	07FC003	Blueberry River below Aitken Creek	BC	1,770	56.677	−121.221
42	07FB001	Pine River at East Pine	BC	12,100	55.718	−121.212
43	08LG008	Spius Creek near Canford	BC	775	50.135	−121.030
44	07FC001	Beatton River near Fort St. John	BC	15,600	56.280	−120.700
45	07FD001	Kiskatinaw River near Farmington	BC	3,630	55.957	−120.563
46	08NL007	Similkameen River at Princeton	BC	1,810	49.460	−120.502
47	08LA001	Clearwater River near Clearwater Station	BC	10,300	51.649	−120.066
48	08NL004	Ashnola River near Keremeos	BC	1,050	49.209	−119.990
49	08LB047	North Thompson River at Birch Island	BC	4,490	51.603	−119.915
50	08LE031	South Thompson River at Chase	BC	15,800	50.765	−119.740
51	07FD009	Clear River near Bear Canyon	AB	2,878.6	56.308	−119.681
52	08LD001	Adams River near Squilax	BC	3,210	50.938	−119.654
53	07GD001	Beaverlodge River near Beaverlodge	AB	1,610	55.189	−119.437
54	08KA007	Fraser River at Red Pass	BC	1,710	52.986	−119.007
55	07GE001	Wapiti River near Grande Prairie	AB	11,300	55.071	−118.803
56	08NN002	Granby River at Grand Forks	BC	2,060	49.044	−118.439
57	07GF001	Simonette River near Goodwin	AB	2,037.6	55.140	−118.182
58	08ND013	Illecillewaet River at Greeley	BC	1,150	51.014	−118.083
59	07AA002	Athabasca River near Jasper	AB	3,872.7	52.910	−118.059

(continued)

TABLE 1. Continued

ID	WSC Code	Gauge Name	Province	Drainage Area	Latitude	Longitude
60	07HA005	Whitemud River near Dixonville	AB	2,019.8	56.511	−117.661
61	07GJ001	Smoky River at Watino	AB	50,300	55.715	−117.623
62	07HC001	Notikewin River at Manning	AB	4,678.8	56.920	−117.618
63	08NJ013	Slocan River near Crescent Valley	BC	3,330	49.461	−117.564
64	08NE074	Salmo River near Salmo	BC	1,240	49.047	−117.294
65	07GG001	Waskahigan River near the mouth	AB	1,040	54.752	−117.206
66	07GG002	Little Smoky river at Little Smoky	AB	3,007.1	54.740	−117.180
67	08NB005	Columbia River at Donald	BC	9,700	51.483	−117.179
68	07GG003	Iosegun River near Little Smoky	AB	1,950	54.745	−117.152
69	07HA003	Heart River near Nampa	AB	1,968.1	56.056	−117.130
70	08NH119	Duncan River below B.B. Creek	BC	1,310	50.638	−117.047
71	08NA002	Columbia River at Nicholson	BC	6,660	51.244	−116.913
72	05DA006	North Saskatchewan River at Saskatchewan Crossing	AB	1,290	51.967	−116.725
73	07AF002	McLeod River above Embarras River	AB	2,561.6	53.470	−116.632
74	07BF002	West Prairie River near High Prairie	AB	1,151.8	55.448	−116.493
75	05DA009	North Saskatchewan River at Whirlpool Point	AB	1,923.2	52.001	−116.471
76	07BF001	East Prairie River near Enilda	AB	1,466.6	55.418	−116.340
77	05DC010	North Saskatchewan River below Bighorn Plant	AB	3,890	52.310	−116.323
78	07AH003	Sakwatamau River near Whitecourt	AB	1,145.1	54.201	−115.779
79	05DC002	North Saskatchewam River at Saunders	AB	5,160	52.453	−115.756
80	05BB001	Bow River at Banff	AB	2,209.6	51.172	−115.572
81	05DC006	Ram River near the mouth	AB	1,853.6	52.368	−115.422
82	07BJ001	Swan River near Kinuso	AB	1,900.4	55.316	−115.417
83	07BB002	Pembina River near Entwistle	AB	4,401.6	53.604	−115.005
84	05DC001	North Saskatchewan River near Rocky Mountain House	AB	11,006.8	52.377	−114.941
85	07AH001	Freeman River near Fort Assiniboine	AB	1,661.7	54.365	−114.905
86	08NK016	Elk River near Natal	BC	1,840	49.866	−114.868
87	05BJ004	Elbow River at Bragg Creek	AB	790.8	50.949	−114.571
88	05AA008	Crowsnest River at Frank	AB	402.7	49.597	−114.411
89	07BK005	Saulteaux River near Spurfield	AB	2,595.6	55.157	−114.239
90	07BK007	Driftwood River near the mouth	AB	2,100.4	55.255	−114.231
91	05AA023	Oldman River near Waldron's Corner	AB	1,446.1	49.814	−114.183
92	05AA022	Castle River near Beaver Mines	AB	820.7	49.489	−114.144
93	05CB001	Little Red Deer River near the mouth	AB	2,578.3	52.028	−114.140
94	05CC001	Blindman River near Blackfalds	AB	1,795.9	52.354	−113.795
95	05DF910[1]	North Saskatchewan River at Devon	AB	NA	53.363	−113.732
96	05FA001	Battle River near Ponoka	AB	1,821.5	52.663	−113.581
97	05DF001	North Saskatchewan River at Edmonton	AB	28,096	53.537	−113.486
98	05EA001	Sturgeon River near Fort Saskatchewan	AB	3,247.1	53.838	−113.282
99	05AE005	Rolph Creek near Kimball	AB	222.4	49.125	−113.143
100	07KE001	Birch River below Alice Creek	AB	9,856.4	58.325	−113.065
101	11AA032	North Fork Milk River above St. Mary Canal	Montana	157.6	48.964	−113.062
102	05CE002	Kneehills Creek near Drumheller	AB	2,428.6	51.469	−112.978
103	07CA005	Pine Creek near Grassland	AB	1,456.4	54.820	−112.778
104	06AA002	Amisk River at Highway No. 36	AB	2,495.9	54.475	−112.014
105	05FB002	Iron Creek near Hardisty	AB	3,500.3	52.708	−111.310
106	06AB001	Sand River near the mouth	AB	4,910.9	54.467	−111.188
107	05AF010	Manyberries Creek at Brodin's Farm	AB	338	49.358	−110.725
108	06AD006	Beaver River at Cold Lake Reserve	AB	14,504.6	54.355	−110.217
109	05EF001	North Saskatchewan River near Deep Creek	SK	57,153.4	53.523	−109.618
110	05EF004	Monnery River near Paradise Hill	SK	875	53.541	−109.527
111	06BA002	Dillon River below Dillon Lake	SK	2,330	55.710	−109.386
112	05EF005	Big Gully Creek near Maidstone	SK	1,620	53.244	−109.296
113	06AF005	Waterhen River near Goodsoil	SK	7,760	54.446	−109.223
114	07MB001	MacFarlane River at outlet of Davy Lake	SK	9,120	58.967	−108.175
115	06BD001	Haultain River above Norbert River	SK	3,680	56.244	−106.561
116	05GF001	Shell Brook near Shellbrook	SK	2,560	53.253	−106.386
117	05GF002	Sturgeon River near Prince Albert	SK	5,100	53.213	−105.885
118	11AE008	Poplar River at International Boundary	Montana	928	48.991	−105.696
119	05GG010	Garden River near Henribourg	SK	903	53.394	−105.611

(continued)

TABLE 1. Continued

ID	WSC Code	Gauge Name	Province	Drainage Area	Latitude	Longitude
120	05JJ009	Saline Creek near Nokomis	SK	950	51.416	−105.103
121	06DA004	Geiki River below Wheeler River	SK	7,730	57.589	−104.203
122	05KB003	Carrot River near Armley	SK	4,400	53.136	−104.021
123	05KF001	Ballantyne River above Ballantyne Bay	SK	1,870	54.561	−103.942
124	05JM010	Ekapo Creek near Marieval	SK	1,100	50.530	−102.710
125	05MC001	Assiniboine River at Sturgis	SK	1,930	51.940	−102.547
126	05LC001	Red Deer River near Erwood	SK	11,000	52.859	−102.195
127	05LE008	Swan River near Norquay	SK	1,920	51.998	−102.074

[1]Not a WSC gauge.

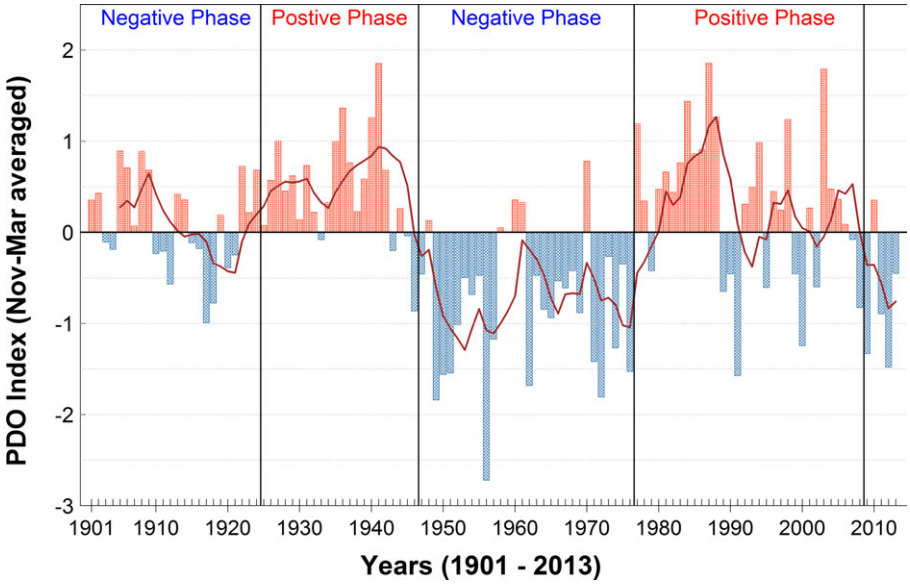

FIGURE 3. Variability in the Pacific Decadal Oscillation (PDO) as Represented by the November to March Averaged PDO Index for the Period 1901-2013, together with the Five-Year Running Mean (dark red line).

TABLE 2. List of El Niño (SOI ≤ −0.5) and La Niña (SOI ≥ 0.5) Events during 1900-2013 as Identified by the June to November Averaged Southern Oscillation Index (SOI).

El Niño Events	La Niña Events
1911, 1912, 1913, 1914, 1918, 1919, 1923, 1925, 1932, 1939, 1940, 1941, 1946, 1951, 1953, 1957, 1963, 1965, 1969, 1972, 1976, 1977, 1982, 1987, 1991, 1992, 1993, 1994, 1997, 2002, 2004, 2006	1910, 1915, 1916, 1917, 1921, 1924, 1938, 1947, 1950, 1955, 1956, 1964, 1970, 1971, 1973, 1974, 1975, 1988, 1996, 1998, 2000, 2008, 2010, 2011

(Chambers *et al.*, 1983; Helsel and Hirsch, 2002). For each of the 127 gauges, the ranked floods (quantiles) of the negative PDO phase (y-axis) were plotted against the ranked floods (quantiles) of the positive PDO phase (x-axis) (i.e., for an individual point (x_i, y_i) of the plot, x_i is the peak flow of the ith ranked flood in the positive PDO phase, and y_i is the peak flow of the ith ranked flood in the negative PDO phase). If the data length of peak flows is same for both phases, the peak flows were directly plotted against each other. If the datasets are not of equal size, the quantiles were picked to correspond to the sorted values from the smaller dataset and then quantiles for the larger dataset were interpolated. The datasets can be assumed to be from the same population if the points fall along the 1:1 line. If the ratio $r_i = (y_i/x_i)$ of the ith ranked floods is > 1, then the ith ranked flood in the negative PDO phase is higher than that in the positive PDO phase. Values of $r_i < 1$ indicate that the ith ranked flood in the positive PDO phase is higher than that in the negative PDO phase. If the PDO phase has no effect on the magnitudes of the floods, the mean ratio R for a given gauge should be approximately 1. For each record, we tested the significance of R at the 0.1 level using a

two-sided permutation test with 10,000 iterations (Text S1) (Manly, 2007).

The impact of the PDO on peak flows also was investigated using flood frequency curves fitted to the annual peak flow series stratified according to PDO phases, and 90% confidence intervals were constructed (USGS, 1982) for all 127 records. If the 90% confidence intervals of the flood frequency curves separate, it cannot be assumed that the annual peak flow series is *i.i.d.* (Franks and Kuczera, 2002). The Kolmogorov-Smirnov goodness-of-fit test was used to determine the probability distribution that best represents the annual peak flow series. EasyfitXL 5.5® was used to test six distributions: the Generalized Extreme Value, 2 & 3 Parameter Lognormal (LN & LN3), Log-Pearson III (LP3), and 2 & 3 Parameter Log-Logistic (LL & LL3). This analysis (Supplementary Table S2) showed that the peak flow series in this region are generally best represented by the LP3 distribution, which is also recommended by the United States Geological Survey (USGS) for defining flood series in the adjacent United States (USGS, 1982; Opere *et al.*, 2006).

Next, to further evaluate if the magnitude of peak flows differ between phases of the PDO, we computed the ratio of the flood (fitted) quantiles in the negative phase to flood quantiles in the positive phase for selected return periods, 2, 5, 10, 25, and 50 years. If this ratio, termed the flood ratio (Franks and Kuczera, 2002; Micevski *et al.*, 2006), is > 1, it may be assumed that the higher magnitude peaks are more common in the negative PDO phase. In this analysis, we expect that peaks will be higher in the negative phase because it is known that total annual discharge is higher in this phase (St. Jacques *et al.*, 2010, 2014; Whitfield *et al.*, 2010). This was done for all the records that Spearman's rank correlation coefficient ρ showed a significant relationship between the PDO and peak flows.

Flood quantiles estimated through flood frequency analysis, using the data from an individual gauge, can have limited predictive value, whereas a regional flood frequency analysis gives more stable and reliable flood quantiles (Lettenmaier *et al.*, 1987; Cunnane, 1988; Hosking and Wallis, 1997). Therefore, the regional index (RI) approach developed by Franks (2002) was applied to the NSRB to explore its characteristics in further detail. We concentrated on this watershed because the naturalized streamflow datasets from Alberta Environment are available for two phases of the PDO, providing sufficient data for this modeling approach. Unfortunately, most of the gauges from the other watersheds do not have continuous and long enough records to perform such a regional frequency analysis. The log-normalized annual peak flow series from the eight gauges (Equation 1), within the NSRB, were collapsed into a single regional index time series by averaging (Equation 2).

$$x_t^j = \frac{\ln Q_t^j}{\sum_{t=1}^{n} \frac{\ln Q_t^j}{n}} \tag{1}$$

$$RI_t = \sum_{j=1}^{m} \frac{x_t^j}{m} \tag{2}$$

Where x_t^j and Q_t^j are the normalized index and annual peak flow, respectively, at gauge j occurring in year t, n is the length of annual peak flow record at each selected gauge, RI_t is the regional index for the year t, and m is the total number of gauges. The series of the regional indices was then stratified according to the PDO phases and the LP3 distribution was used to construct the flood frequency curves.

RESULTS AND DISCUSSION

The PDO has a definite impact on flood magnitudes in western Canada. Spearman's rank correlation coefficient ρ shows that a significant relationship exists between the winter PDO index and peak flow magnitude for 38% of the gauges examined (48 of the 127 records) (Figure 4A). These gauges show a negative relationship between the winter PDO and flood magnitude, that is, floods are higher during the negative PDO phase than during the positive PDO phase. There is a single exception where a positive relationship exists, the gauge 08FF001 (Kitimat River below Hirsch Creek). The gauges showing a significant negative relationship are concentrated in the Fraser River Basin, southern British Columbia, the mountain headwaters of the South and North Saskatchewan River Basins, and the Peace River Basin, with a few scattered gauges in central Saskatchewan. In particular, the western half of the proposed path of the Northern Gateway Pipeline runs through the upper Fraser Valley, British Columbia, where the PDO phase has a clear impact on the peak flows as shown by Spearman's ρ. The positive relationship at coastal Kitimat is unsurprising because the relationship between the PDO and total winter precipitation becomes a positive one in central and northern coastal British Columbia and northeastern Saskatchewan (Figure S3). Throughout the rest of the study area, there is a negative relationship between the PDO and total winter precipitation. We also ran

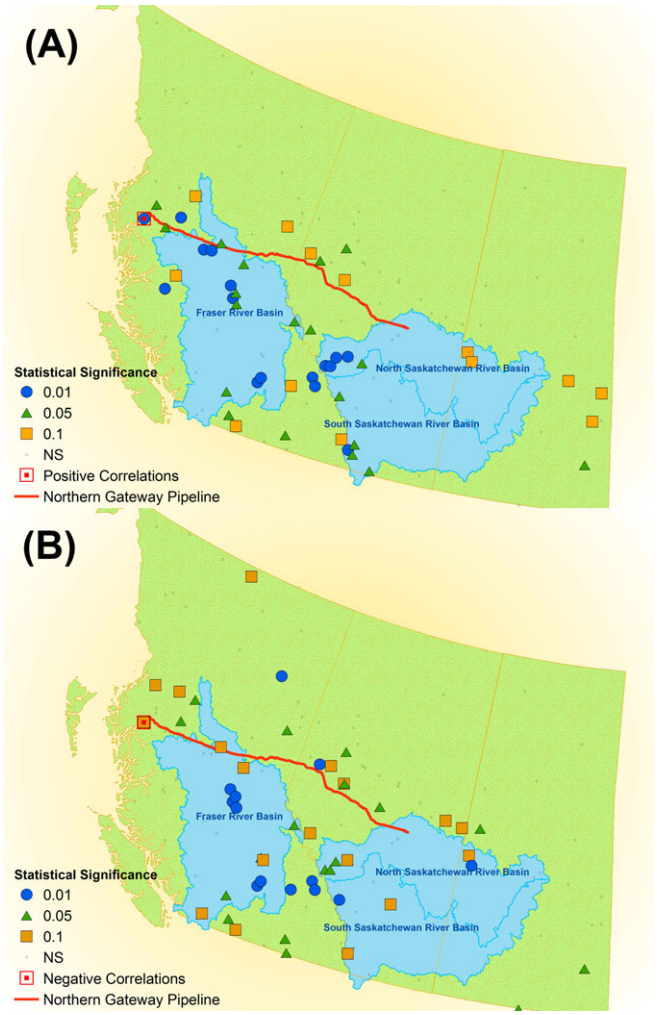

FIGURE 4. (A) Geographical Pattern of the Significant Spearman's Rank Correlation Coefficients ρ between Peak Flows at the 127 Gauges and the Winter (November-March) Pacific Decadal Oscillation (PDO) Index. (B) Geographical pattern of the significant Spearman's rank correlation coefficients ρ between peak flows at the 127 gauges and the previous year's June-November Southern Oscillation Index (SOI). Significant relationships are shown by large colored symbols. NS denotes not significant. Significant correlations denote a negative relationship for the PDO unless denoted otherwise, and a positive relationship for the SOI unless denoted otherwise.

Spearman's rank correlation coefficients for the fixed time period 1961-2010 and found almost identical results (results not shown). To the best of our knowledge, this study is the first to examine in detail the effect of the PDO on flood magnitudes in western Canada. Sharif and Burn (2009) examined the effect of the PDO on 62 Reference Hydrological Basin Network (RHBN) stations across all Canada and found that 3 stations were affected by the positive phase of the PDO and 5 by the negative phase across the entire country. Unfortunately, they give neither the location of these stations, nor the sign of the relationships.

Similar to the PDO, ENSO has a clear impact on these same flood magnitudes. Spearman's ρ shows that a significant positive relationship exists between the SOI and peak flow magnitude for 39% of the gauges examined (49 of 127 records) (Figure 4B). Thus, floods are higher during La Niña events than during El Niño events. Again, the gauge 08FF001 (Kitimat River) is the exception with a negative relationship instead. The geographic pattern is similar to that from the PDO, although not identical. Woo and Thorne (2003) examined 110 stations spread across British Columbia, Alberta, and Saskatchewan to analyze the effect of ENSO on annual peak flows for 1968-1998 and identified that 34% (37 of 110) of the stations show statistically significant relations with the October-March averaged SOI. Our analysis shows a slightly stronger impact of ENSO on peak flows (i.e., a higher percentage of gauges) than that of Woo and Thorne (2003) for two possible reasons: (1) we are analyzing longer full period of record datasets and (2) although we both use the SOI, we are using different definitions of ENSO events. We follow the definition of Redmond and Koch (1991) who examined the SOI to determine the definition of ENSO events that produced the strongest teleconnection pattern for the Pacific Northwest region. That the spatial pattern and sign of the PDO's effect is so similar to that of ENSO is expected, given that it is thought that the PDO is not a primary mode of variability, but rather a function of multiple interacting climate processes, including ENSO, mid-latitude atmospheric influences on sea surface temperature (SST), and mid-latitude ocean circulation (e.g., the Kuroshio Current) (Alexander, 2010). Consequently, El Niño events are more likely to occur during the positive PDO phase and La Niña events are more likely to occur during the negative PDO phase (Kiem *et al.*, 2003; St. Jacques *et al.*, 2014).

The Q-Q plots also present evidence that PDO phase has a clear impact on peak flood magnitudes. Figure 5 shows the Q-Q plots for the 48 gauges that showed a significant relationship between the winter PDO index and annual peak flows according to Spearman's ρ (Figure 4A). These Q-Q plots confirm that it is unlikely that the annual peak flows are identically distributed regardless of the PDO phase since there are few gauges where the quantiles fall along the 1:1 line (Figure 5). The Q-Q plots demonstrate that higher magnitude floods are typically more common during the negative PDO phase, since the flood quantiles largely appear above the 1:1 line. The permutation tests show that this is a significant result ($p < 0.1$) for 39 of the 48 records. Again, the Kitimat River (08FF001) is the exception where the

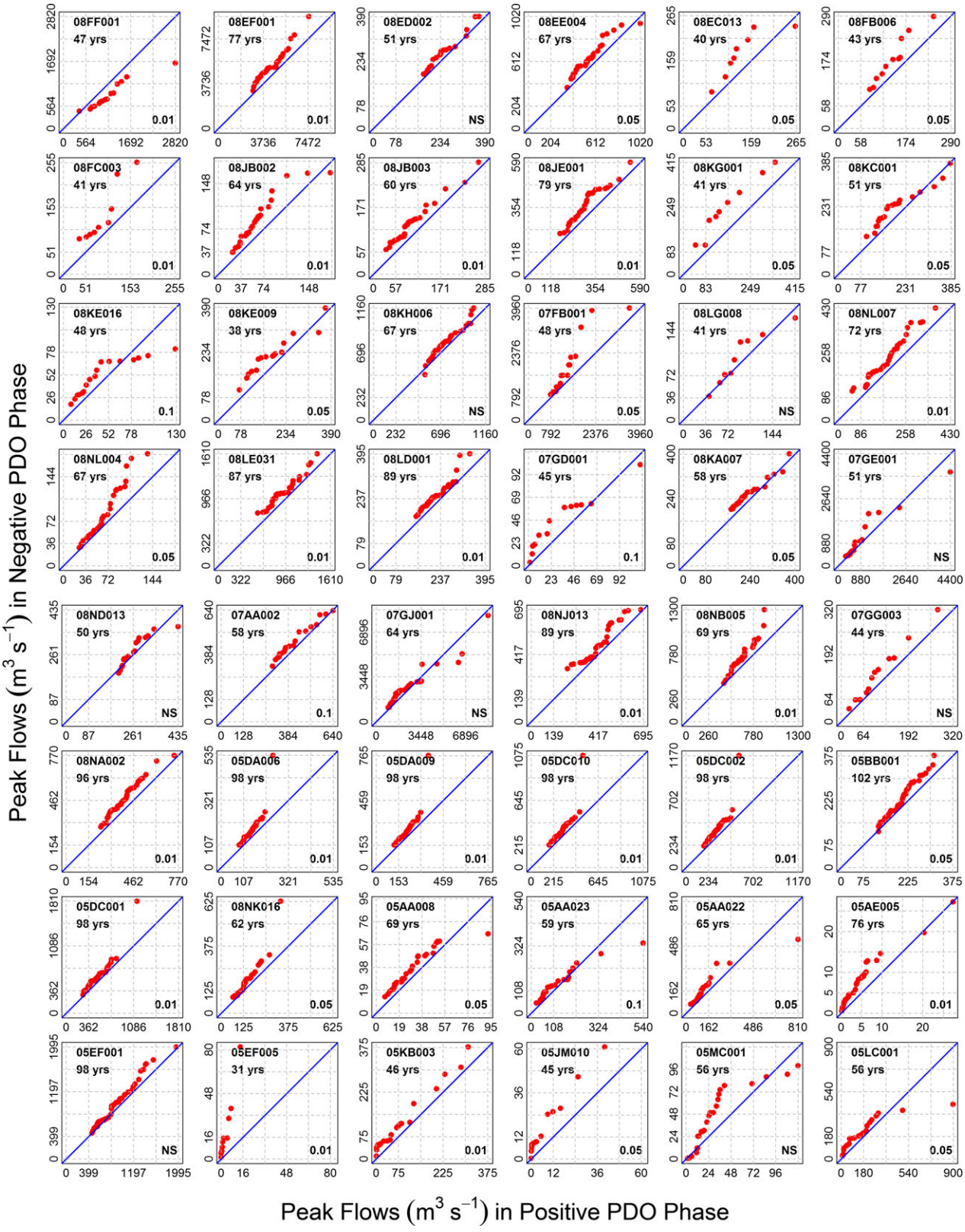

FIGURE 5. Quantile-Quantile (Q-Q) Plots Based on the Annual Peak Flows ($m^3 s^{-1}$) Stratified According to Pacific Decadal Oscillation (PDO) Phase, for the 48 Streamflow Gauges in Western Canada That Spearman's Rank Correlation Coefficient ρ Shows a Significant Relationship between PDO Phase and Peak Floods. Shown in blue are the 1:1 lines. WSC station codes are shown in the upper left hand corners, together with record length. Shown in the lower right hand corners are the significance levels of the permutation test. NS denotes not significant.

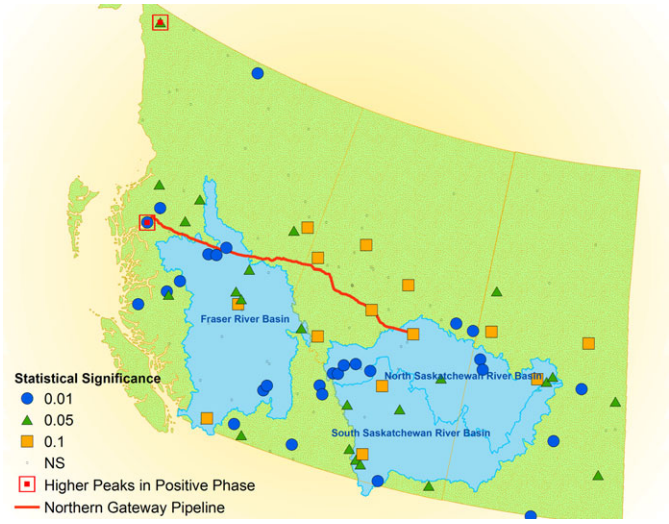

FIGURE 6. Geographical Pattern of the Significant Permutation Tests on the Quantile-Quantile (Q-Q) Plots Exploring the Relationship between Peak Flows at the 127 Gauges and the Winter (November-March) Pacific Decadal Oscillation (PDO) Index. Significant relationships are shown by large colored symbols. NS denotes not significant. Significant correlations denote a negative relationship unless denoted otherwise.

points fall significantly below the 1:1 line, that is, higher magnitude floods are more common during the positive phase of the PDO. An additional 26 gauges that did not show a relationship between the PDO and peak flow according to Spearman's ρ, do show a significant relationship according to the permutation tests on the Q-Q plots, giving a total of 51% (65 of 127) of the gauges (Figure 6 and Figure S4). The geographical pattern of these 65 gauges is broadly similar to that of the 48 gauges significant by Spearman's ρ, but it is denser and shows a much greater impact of the PDO in central and southern Alberta and Saskatchewan. The positive relationship between the PDO and flood magnitudes at the coastal Kitimat and Atlin Rivers in British Columbia are unsurprising because the relationship between the PDO and total winter precipitation becomes a positive one here (Figure S3).

Similarly, flood frequency analysis presents further evidence that it is unlikely that the annual peak flows are *i.i.d.* regardless of the PDO phase, although it is more mixed. Some records, for example, the North Saskatchewan River at Saunders (05DC002), show a complete separation of the confidence intervals of the flood frequency curves stratified by PDO phase (Figure 7A). Other records showed only partial separation. For example, Figures 7B and 7C show the stratified flood frequency curves for the still naturally flowing headwaters of the Columbia River at Nicholson (08NA002) and Donald (08NB005), British Columbia. They indicate that the annual peak flows in the negative PDO phase are not identical to those of the positive phase, since at Nicholson the confidence intervals separate at higher frequencies or lower return periods, and at Donald the confidence intervals separate at lower frequencies or higher return periods. Of the 48 records that showed the impact of the PDO on peak flows using Spearman's ρ, 8% showed clearly separated flood frequency curves and confidence intervals, 29% showed separation at higher frequencies, 6% showed separation at lower frequencies, and 54% showed no separation (e.g., Figure 7D — the Bow River at Banff (05BB001)). Many of the records that showed no separation of the confidence intervals still showed more frequent higher magnitude floods during the negative PDO, for example, the Oldman River at Waldron's Corner (results not shown). Overall, FFA was hampered by the shortness of peak flow record lengths in western Canada (the records had an average length of 52 years) (Table S1). As well, longer record lengths would improve the accuracy of the tails of the stratified flood frequency curves. The flood records were of relatively short length (an average of 58 years) in the upper Fraser River Valley (the location of the proposed Northern Gateway Pipeline), which precluded the use of the regional index approach and made FFA at individual gauges problematic (Table S1).

Even though only slightly less than half the records have stratified flood frequency curves with confidence intervals that show some separation, the following results still suggest that the impact of PDO phase on annual peak flows can be detected using FFA curves. Figure 8 shows the histogram of the flood ratios for the 48 gauges that show a significant relationship between the PDO index and annual peak flow according to Spearman's ρ (Figure 4A). If the annual floods in both the PDO phases were *i.i.d.*, ~50% of the gauges would have a flood ratio ≤ 1 (Micevski *et al.*, 2006). However, the flood ratios for the return period of 25 years is ≤ 1 for 21% of the gauges (Figure 8). For the 50-year return period, 27% of the gauges have flood ratios ≤ 1, which again is much less than the 50% threshold (Figure 8). The mean of the flood ratios at the 48 gauges is > 1.23 for all the return periods (Table 3). Although the flood ratios have a wide spread (as shown by their standard deviations) at shorter return periods, the results indicate strong differences in annual flood quantiles dependent on PDO phase, providing further evidence that the annual floods are not identically distributed.

Focusing on the economically important NSRB with its longer records spanning approximately two PDO cycles (an average length of 98 years) (Table S1), a regional index (RI) was computed based on the annual peak flow data from the eight NSRB gauges, and flood frequency curves were fit along with 90% confidence intervals to the stratified RI

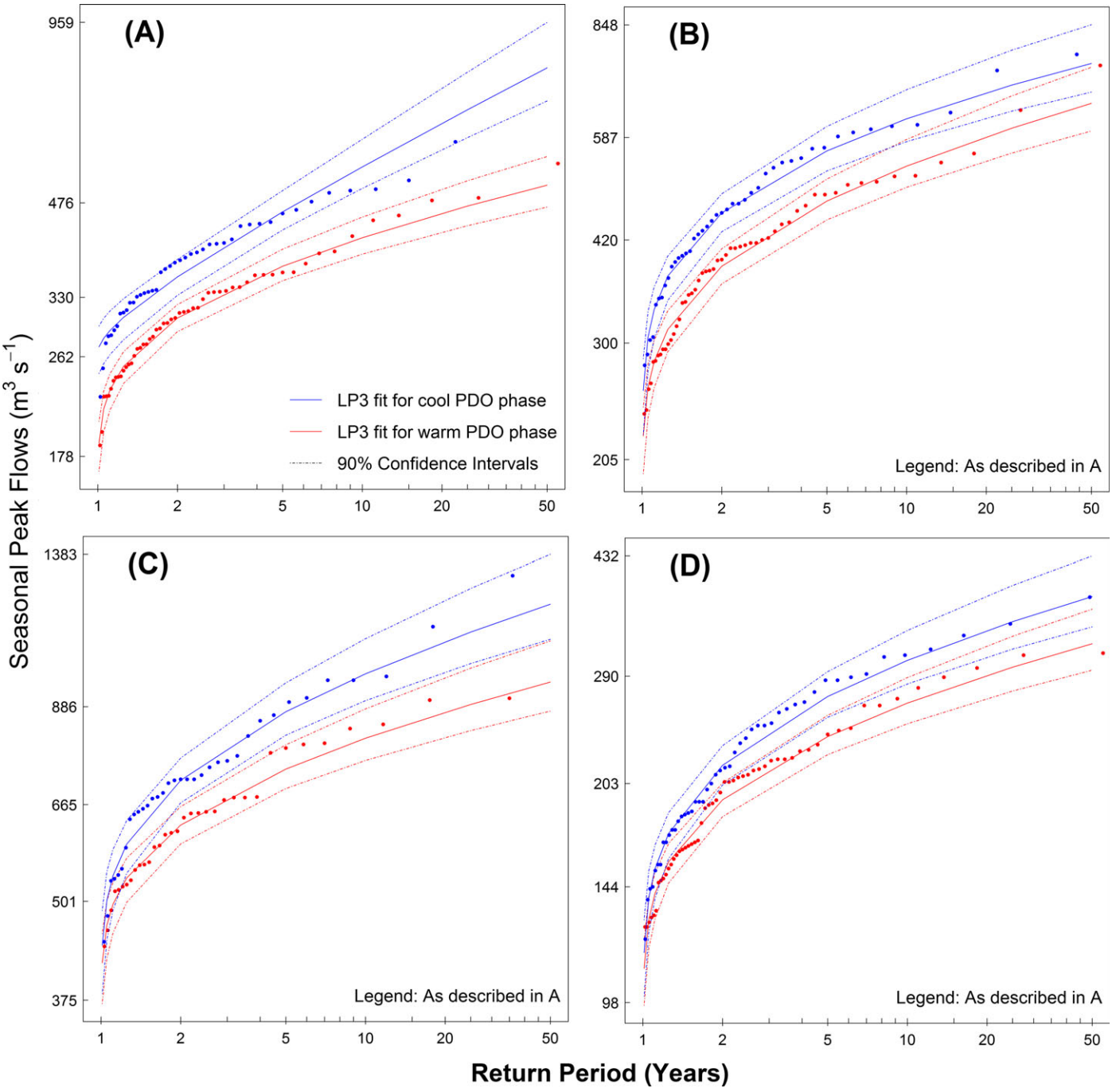

FIGURE 7. Log-Pearson III (LP3) Expected Quantiles and Their 90% Confidence Intervals (dashed lines) for the Annual Peak Flows for Selected Rivers, Stratified According to Cool (1905-1924, 1947-1976, 2009-2013) and Warm (1925-1946, 1977-2008) Phases of the Pacific Decadal Oscillation (PDO). (A) North Saskatchewan River at Saunders (05DC002), (B) Columbia River at Nicolson (08NA002), (C) Columbia River at Donald (08NB005), and (D) Bow River at Banff (05BB001).

series (Figure 9). These results show that the annual peak flows from the NSRB stratified according to PDO phase are not *i.i.d.* The flood frequency confidence intervals separate for return periods > 4 years, and the negative PDO phase produces significantly higher magnitude floods occurring at greater frequency compared to those in the positive phase.

We explored creating a similar regional index for the equally economically important South Saskatchewan River Basin (SSRB), a premier agricultural region of Canada, which is heavily dependent on SSRB surface flows for irrigation (Figure 4A). This region is under such severe demand for surface water supplies that large portions of the SSRB have been

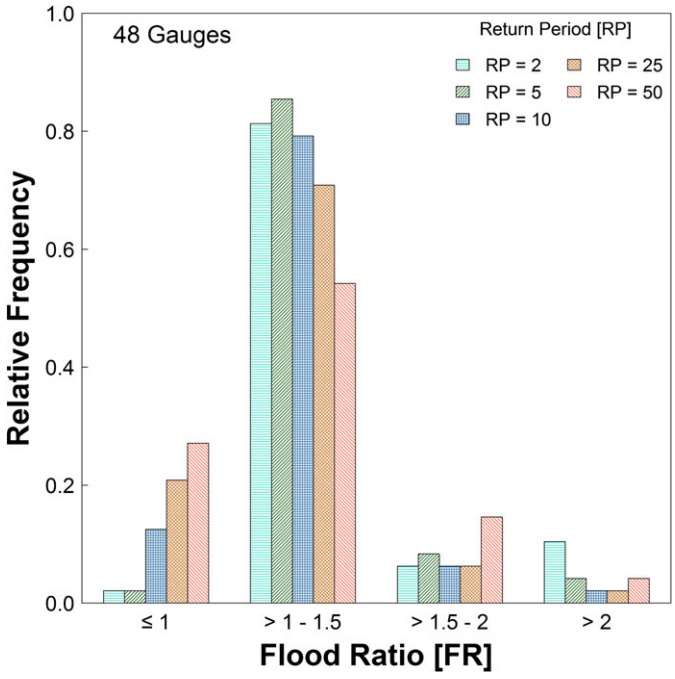

FIGURE 8. Histogram of Flood Ratios (FR) for Return Periods (RP) between 2 and 50 Years for the 48 Western Canadian Rivers that Show a Significant Relationship between the PDO Index and Annual Peak Flow According to Spearman's Rank Correlation Coefficient ρ (see Figure 4A).

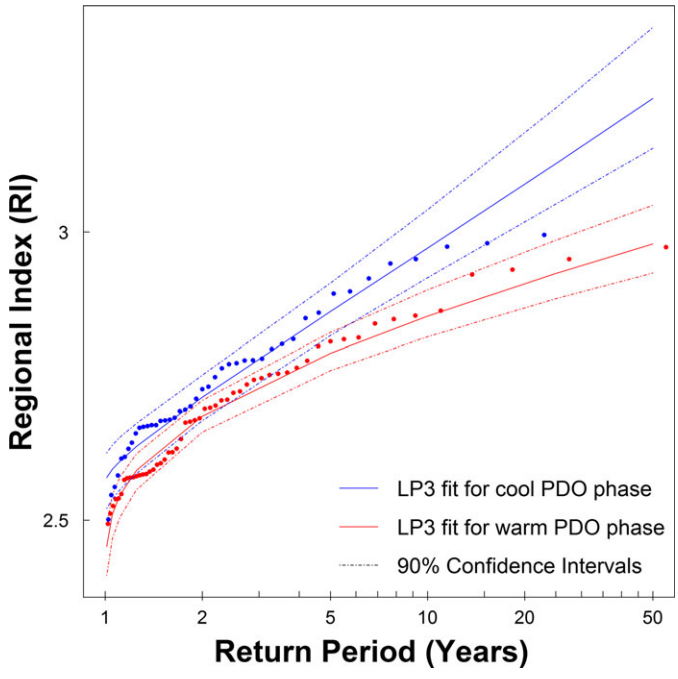

FIGURE 9. Log-Pearson III (LP3) Flood Frequency Curves and Their 90% Confidence Intervals (dashed lines) for the Regional Index of the Annual Peak Flow Series from the Eight North Saskatchewan River Basin (NSRB) Rivers Stratified According to the Negative (1912-1924, 1947-1976, 2009-2013) and Positive (1925-1946, 1977-2008) Phases of the Pacific Decadal Oscillation (PDO).

TABLE 3. Means and Standard Deviations of the Flood Ratios (Ratios of the Fitted Flood Quantiles in the Negative and Positive PDO Phases) for Selected Return Periods at the 48 Gauges in Western Canada that Show a Significant Relationship between the PDO Index and Annual Peak Flow According to Spearman's Rank Correlation Coefficient ρ (see Figure 4A).

	Flood Ratio (FR)	
Return Period (RP)	**Mean**	**Standard Deviation**
2	1.52	1.18
5	1.33	0.64
10	1.27	0.56
25	1.24	0.58
50	1.23	0.63

closed to further allocation (Rood and Vandersteen, 2010; Sauchyn *et al.*, 2016). It was also severely impacted by the June 2013 southern Alberta floods, heightening interest in more accurate flood frequency curves. This flooding is the costliest natural disaster in Canadian history, estimated at more than $1.7 billion of insured damage (Calgary Sun, Insurance Bureau of Canada says $1.7 billion southern Alberta flood costliest disaster in Canadian history. Published on 23rd September, 2013, http://www.calgarysun.com/2013/09/23/insurance-bureau-of-canada-says-17-billion-southern-alberta-flood-costliest-disaster-in-canadian-history). We concluded that there was neither a set of high-enough quality naturalized peak flow records, nor a large enough set of mixed naturally flowing and regulated gauge records that were free enough of the effects of dam construction in this heavily humanly modified region. Unfortunately, many dams were constructed here at the same time as PDO phase changes, making it difficult to separate out the effects of the PDO phase *vs.* that of dam construction for flood control.

There is accumulating worldwide evidence that flood magnitudes and frequencies are affected by the major climate oscillations such as the PDO and ENSO. The effects of the PDO on floods in western Canada are similar to those observed in eastern Australia from the Inter-decadal Pacific Oscillation (IPO) (Franks, 2002; Franks and Kuczera, 2002; Kiem *et al.*, 2003). Similar to the role of the PDO in western Canada, the flood risk in eastern Australia is higher when the IPO is in a negative *vs.* positive phase. The IPO is closely related to the PDO, if not its pan-Pacific manifestation (Folland *et al.*, 1999; Franks, 2002; Kiem *et al.*, 2003). Franks and Kuczera (2002) and Kiem *et al.* (2003) also demonstrated that flood frequency in eastern Australia is impacted by

ENSO. Ward *et al.* (2014) determined that La Niña events produce higher annual floods compared to El Niño events in the majority of the world's river basins. Andrews *et al.* (2004) determined that El Niño events produced higher annual floods along the California coast.

CONCLUSIONS

Knowledge of the magnitude and frequency of floods is necessary in the planning and design of infrastructure and adaptive water management policy. Results such as ours and Franks (2002), Franks and Kuczera (2002), Kiem *et al.* (2003), Andrews *et al.* (2004), and Ward *et al.* (2014) highlight the potential inadequacy of widely used, traditional FFA with its primary assumption of *i.i.d.* peak annual flows. Kwon *et al.* (2008), Stedinger and Griffis (2008, 2011), López and Francès (2013), and Barros *et al.* (2014) argue that the *i.i.d.* assumption can no longer be considered valid. Therefore, knowledge of climate state with regard to teleconnection patterns should be considered before performing FFA. However, almost all FFA done in Canada invokes the *i.i.d.* assumption (e.g., Neill and Watt, 2001; Aucoin *et al.*, 2011). Our results suggest that the *i.i.d.* assumption is not tenable in western Canada where the hydroclimatology is strongly influenced by the low-frequency PDO (Mantua *et al.*, 1997; Rood *et al.*, 2005; Gobena and Gan, 2006; Wang *et al.*, 2006; Fleming *et al.*, 2007; Fleming and Whitfield, 2010; St. Jacques *et al.*, 2010, 2014; Whitfield *et al.*, 2010). In particular, the upper Fraser River Basin (the pathway of the proposed Northern Gateway pipeline), the Columbia River Basin, and the North Saskatchewan River Basin are subregions where the *i.i.d.* assumption seems dubious. Ignoring the multi-decadal variability of large-scale climate states here could lead to flood risk underestimation, and under-design and under-construction of key infrastructure. The extent of this problem remains to be explored; it is manifest in western Canada, California, and eastern Australia (this study; Franks, 2002; Franks and Kuczera, 2002; Kiem *et al.*, 2003; Woo and Thorne, 2003; Andrews *et al.*, 2004; Ward *et al.*, 2014). Any region with a strong teleconnection with the PDO or IPO may be subject to flood risk underestimation arising in this fashion. Furthermore, other regions with strong teleconnections to other atmosphere-ocean oscillations, for example, the North Atlantic Oscillation or the Atlantic Multi-decadal Oscillation, may also be at risk.

DATA AVAILABILITY

Observed streamflow data are publicly available at the WSC database: http://www.ec.gc.ca/rhc-wsc/default.asp?lang=En&n=9018B5EC-1. Naturalized weekly streamflow data are obtained from Alberta Environment and Parks: http://esrd.alberta.ca.

SUPPORTING INFORMATION

Additional supporting information may be found online under the Supporting Information tab for this article: A detailed map of streamflow gauges with the major rivers shown, a plot of ENSO variability, a map of Spearman's rank correlations (ρ) between annual peak flow & PDO, and additional significant Q-Q plots; a table of streamflow gauges with additional details, a table of the best fits of the distributions to the annual peak flow data, and a table of Spearman's rank correlations (ρ) are added; and an R-script is provided to perform permutation tests on the Q-Q plots for significance.

LITERATURE CITED

Alexander, M.A., 2010. Extratropical Air-Sea Interaction, SST Variability and the Pacific Decadal Oscillation (PDO). *In*: Climate Dynamics: Why Does Climate Vary, D. Sun and F. Bryan (Editors). AGU Monograph #189, Washington, D.C., pp. 123-148.

Andrews, E.D., R.C. Antweiler, P.J. Neiman, and F.M. Ralph, 2004. Influence of ENSO on Flood Frequency Along the California Coast. Journal of Climate 17(2):337-348, DOI: 10.1175/1520-0442(2004) 017%3C0337:IOEOFF%3E2.0.CO;2.

Aucoin, F., D. Caissie, N. El-Jabi, and N. Turkkan, 2011. Flood Frequency Analysis for New Brunswick Rivers. Canadian Technical Report of Fisheries and Aquatic Sciences 2920, 77 p., ISSN: 0706-6457

Barros, A.P., Y. Duan, J. Brun, and M.A. Medina, 2014. Flood Non-Stationarity in the SE and Mid-Atlantic Regions of the United States. Journal of Hydrologic Engineering 19(10):05014014, DOI: 10.1061/(ASCE)HE.1943-5584.0000955.

Bonsal, B. and A. Shabbar, 2008. Impacts of Large-Scale Circulation Variability on Low Streamflows Over Canada: A Review. Canadian Water Resources Journal 33(2):137-154, DOI: 10.4296/cwrj3302137.

Bonsal, B.R. and R.G. Lawford, 1999. Teleconnections between El Niño and La Niña Events and Summer Extended Dry Spells on the Canadian Prairies. International Journal of Climatology 19 (13):1445-1458, DOI: 10.1002/(SICI)1097-0088(19991115) 19:13 < 1445:AID-JOC431 > 3.0.CO;2-7.

Chambers, J.M., W.S. Cleveland, B. Kleiner, and P.A. Tukey, 1983. Graphical Methods for Data Analysis (Statistics). Chapman and Hall/CRC Publishers, Belmont, ISBN 13: 978-0871504135.

Cunnane, C., 1988. Methods and Merits of Regional Flood Frequency Analysis. Journal of Hydrology 100(1-3):269-290, DOI: 10.1016/0022-1694(88)90188-6.

Fleming, S.W. and P.H. Whitfield, 2010. Exploratory Spatiotemporal Mapping of ENSO and PDO Surface Meteorological Signals in British Columbia, Yukon, and Southeast Alaska. Atmosphere-Ocean 48(2):122-131, DOI: 10.3137/AO1107.2010.

Fleming, S.W., P.H. Whitfield, R.D. Moore, and E.J. Quilty, 2007. Regime-Dependent Streamflow Sensitivities to Pacific Climate Modes Across the Georgia-Puget Transboundary Ecoregion. Hydrological Processes 21(24):3264-3287, DOI: 10.1002/hyp.6544.

Folland, C.K., D.E. Parker, A.W. Colman, and R. Washington, 1999. Large Scale Modes of Ocean Surface Temperature Since the Late Nineteenth Century. *In*: Beyond El Niño: Decadal and Interdecadal Climate Variability, A. Navarra (Editor). Springer-Verlag, Berlin Heidelberg, pp. 73-102, DOI: 10.1007/978-3-642-58369-8.

Franks, S.W., 2002. Identification of a Change in Climate State Using Regional Flood Data. Hydrology and Earth System Sciences 6(1):11-16, DOI: 10.5194/hess-6-11-2002.

Franks, S.W. and G. Kuczera, 2002. Flood Frequency Analysis: Evidence and Implications of Secular Climate Variability, New South Wales. Water Resources Research 38(5):20.1-20.7, DOI: 10.1029/2001WR000232.

Gobena, A.K. and T.Y. Gan, 2006. Low-Frequency Variability in Southwestern Canadian Streamflow: Links with Large-Scale Climate. International Journal of Climatology 26(13):1843-1869, DOI: 10.1002/joc.1336.

Helsel, D.R. and R.M. Hirsch, 2002. Statistical Methods in Water Resources. *In*: Book 4 Hydrologic Analysis and Interpretation. Techniques of Water-Resources Investigations Reports, United States Geological Survey (USGS), Chapter A3, Book 4, 524p. http://pubs.usgs.gov/twri/twri4a3/.

Hosking, J.R.M. and J.R. Wallis, 1997. Regional Frequency Analysis. Cambridge University Press, Cambridge, United Kingdom, ISBN 13: 978-0-521-01940-8.

Kiem, A.S., S.W. Franks, and G. Kuczera, 2003. Multi-Decadal Variability of Flood Risk. Geophysical Research Letters 30 (2):1035, DOI: 10.1029/2002GL015992.

Kwon, H.-H., C. Brown, and U. Lall, 2008. Climate Informed Flood Frequency Analysis and Prediction in Montana Using Hierarchical Bayesian Modelling. Geophysical Research Letters 35(5): L05404, DOI: 10.1029/2007GL032220.

Lapp, S.L., J.M. St. Jacques, D.J. Sauchyn, and J.R. Vanstone, 2013. Forcing of Hydroclimatic Variability in the Northwestern Great Plains Since AD 1406. Quaternary International 310 (15):47-61, DOI: 10.1016/j.quaint.2012.09.011.

Lettenmaier, D.P., J.R. Wallis, and E.F. Wood, 1987. Effect of Heterogeneity on Flood Frequency Estimation. Water Resources Research 23(2):313-323, DOI: 10.1029/WR023i002p00313.

López, J. and F. Francès, 2013. Non-Stationary Flood Frequency Analysis in Continental Spanish Rivers, Using Climate and Reservoir Indices as External Covariates. Hydrology and Earth System Sciences 17(8):3189-3203, DOI: 10.5194/hess-17-3189-2013.

Manly, B.F.J., 2007. Randomization, Bootstrap and Monte Carlo Methods in Biology, 3rd edn. Chapman and Hall, London.

Mantua, N.J., S.R. Hare, Y. Zhang, J.M. Wallace, and R.C. Francis, 1997. A Pacific Interdecadal Climate Oscillation with Impacts on Salmon Production. Bulletin of the American Meteorological Society 78(6):1069-1079, DOI: 10.1175/1520-0477(1997) 078 < 1069:APICOW>2.0.CO;2.

Micevski, T., S.W. Franks, and G. Kuczera, 2006. Multidecadal Variability in Coastal Eastern Australian Flood Data. Journal of Hydrology 327(1-2):219-225, DOI: 10.1016/j.jhydrol.2005.11.017.

Minobe, S., 1997. A 50-70 Year Climatic Oscillation Over the North Pacific and North America. Geophysical Research Letters 24 (6):683-686, DOI: 10.1029/97GL00504.

Neill, C.R. and W.E. Watt, 2001. Report on Six Case Studies of Flood Frequency Analyses. Transportation and Civil Engineering Division, Alberta Transportation. http://www.transportation.alberta.ca/Content/doctype30/Production/ffasixcase.pdf, *accessed* March 2012.

Opere, A.O., S. Mkhandi, and P. Willems, 2006. At Site Flood Frequency Analysis for the Nile Equatorial Basins. Physics and Chemistry of the Earth 31(15-16):919-927, DOI: 10.1016/j.pce.2006.08.018.

Redmond, K.T. and R.W. Koch, 1991. Surface Climate and Streamflow Variability in the Western United States and Their Relationship to Large-Scale Circulation Indices. Water Resources Research 27(9):2381-2399, DOI: 10.1029/91WR00690.

Rood, S.B., G.M. Samuelson, J.K. Weber, and K.A. Wywrot, 2005. Twentieth-Century Decline in Streamflows from the Hydrographic Apex of North America. Journal of Hydrology 306 (1-4):215-233, DOI: 10.1016/j.jhydrol.2004.09.010.

Rood, S.B. and J.W. Vandersteen, 2010. Relaxing the Principle of Prior Approximation: Stored Water and Sharing the Shortage in Alberta, Canada. Water Resources Management 24(8):1605-1620, DOI: 10.1007/s11269-009-9516-0.

Sauchyn, D.J., J.-M. St. Jacques, E. Barrow, M.W. Nemeth, R.J. MacDonald, A.M.S. Sheer, and D.P. Sheer, 2016. Adaptive Water Resource Planning in the South Saskatchewan River Basin: Use of Scenarios of Hydroclimatic Variability and Extremes. Journal of the American Water Resources Association 52(1):222-240, DOI: 10.1111/1752-1688.12378.

Shabbar, A., B. Bonsal, and M. Khandekar, 1997. Canadian Precipitation Patterns Associated with the Southern Oscillation. Journal of Climate 10(12):3016-3027, DOI: 10.1175/1520-0442(1997) 010%3C3016:CPPAWT%3E2.0.CO;2.

Shabbar, A. and M. Khandekar, 1996. The Impact of El Niño-Southern Oscillation on the Temperature Field Over Canada. Atmosphere-Ocean 34(2):401-416, DOI: 10.1080/07055900.1996.9649570.

Sharif, M. and D. Burn, 2009. Detection of Linkages between Extreme Flow Measures and Climate Indices. International Journal of Civil, Environmental, Structural, Construction and Architectural Engineering 3(12):495-500, DOI: scholar.waset.org/1999.3/6613.

Stedinger, J.R. and V.W. Griffis, 2008. Flood Frequency Analysis in the United States: Time to Update. Journal of Hydrologic Engineering 13(4):199-204, DOI: 10.1061/(ASCE)1084-0699(2008) 13:4(199).

Stedinger, J.R. and V.W. Griffis, 2011. Getting from Here to Where? Flood Frequency and Climate. Journal of the American Water Resources Association 47(3):506-513, DOI: 10.1111/j.1752-1688.2011.00545.x.

St. Jacques, J.M., Y.A. Huang, Y. Zhao, S.L. Lapp, and D.J. Sauchyn, 2014. Detection and Attribution of Variability and Trends in Streamflow Records from the Canadian Prairie Provinces. Canadian Water Resources Journal 39(3):270-284, DOI: 10.1080/07011784.2014.942575.

St. Jacques, J.M., D.J. Sauchyn, and Y. Zhao, 2010. Northern Rocky Mountain Streamflow Records: Global Warming Trends, Human Impacts or Natural Variability? Geophysical Research Letters 37(6):L06407, DOI: 10.1029/2009GL042045.

Tan, X. and T.Y. Gan, 2015. Nonstationary Analysis of Annual Maximum Streamflow of Canada. Journal of Climate 28 (5):1788-1805, DOI: 10.1175/JCLI-D-14-00538.1.

USGS, 1982. Guidelines for Determining Flood Flow Frequency. Bulletin 17B of the Hydrology Subcommittee, United States Geological Survey (USGS). http://water.usgs.gov/osw/bulletin17b/dl_flow.pdf.

Wang, J.Y., P.H. Whitfield, and A.J. Cannon, 2006. Influence of Pacific Climate Patterns on Low-Flows in British Columbia and Yukon, Canada, Canadian Water Resources Journal 31(1):25-40, DOI: 10.4296/cwrj3101025.

Ward, P.J., S. Eisner, M. Flörke, M.D. Dettinger, and M. Kummu, 2014. Annual Flood Sensitivities to El Niño-Southern Oscillation at the Global Scale. Hydrology and Earth System Sciences 18:47-66, DOI: 10.5194/hess-18-47-2014.

Whitfield, P.H., R.D. (Dan) Moore, S.W. Fleming, and A. Zawadzki, 2010. Pacific Decadal Oscillation and Hydroclimatology of Western Canada – Review and Prospects. Canadian Water Resources Journal 35(1):1-28, DOI: 10.4296/cwrj3501001.

Wilks, D.S., 2006. Statistical Methods in the Atmospheric Sciences, 2nd edn. Elsevier Academic Press, Burlington, United States of America, ISBN 13: 978-0-12-751966-1.

Woo, M. and R. Thorne, 2003. Comment on "Detection of Hydrologic Trends and Variability," by Burn, D.H. and Hag Elnur, M.A., 2002. Journal of Hydrology 255, 107–122. Journal of Hydrology 277(1-2):150-160, DOI: 10.1016/S0022-1694(03)00079-9